Assessment of sensor change on long-term NSIDC DAAC passive microwave sea ice extent climate record

Walt Meier, NSIDC DAAC Scientist 21 June
2026

History of the NSIDC DAAC passive microwave sea ice extent climate record

The passive microwave record of sea ice concentrations has been a mainstay climate record hosted at the NASA Snow and Ice Distributed Active Archive Center (DAAC) at the National Snow and Ice Data Center (NSIDC). The record begins in October 1978 and provides a continuous and nearly complete climate record of sea ice concentration, area (total surface area covered by ice), and extent (area covered by at least 15% concentration ice).

Numerous algorithms have been developed to derive sea ice concentration from input passive microwave brightness temperatures observed by satellite-borne sensors. One of the earliest algorithms is the NASA Team (NT) algorithm, developed by scientists at NASA Goddard Space Flight Center. The NT algorithm has been the source of a long-term sea ice concentration climate record managed by the NSIDC DAAC, "Sea Ice Concentrations from Nimbus-7 SMMR and DMSP SSM/I-SSMIS Passive Microwave Data, Version 2" (NSIDC-0051) (DiGirolamo et al., 2022; https://nsidc.org/data/nsidc-0051/versions/2). It is one of the most visible sea ice concentration products, used in NSIDC's Sea Ice Index (Fetterer et al., 2025; https://nsidc.org/data/seaice_index) and various climate reports, such as the NOAA Arctic Report Card (https://arctic.noaa.gov/report-card/).

The NSIDC-0051 NT product has been updated every 3-12 months by researchers at Goddard. For interim data, the NSIDC DAAC has processed near-real-time NT fields, the NSIDC-0081 product, "Near-Real-Time DMSP SSMIS Daily Polar Gridded Sea Ice Concentrations, Version 2" (Meier et al., 2021; https://nsidc.org/data/nsidc-0081/versions/2).

These sea ice concentration fields have been derived from gridded brightness temperatures (TBs) acquired by a series of satellite sensors, most recently the Special Sensor Microwave Imager and Sounder (SSMIS) on the U.S. Department of Defense Meteorological Satellite Program (DMSP) satellite series. In late April 2025, data gaps started appearing in the SSMIS fields. As a result, the NSIDC DAAC began publishing an NT product based on TBs from the JAXA Advanced Microwave Scanning Radiometer 2 (AMSR2). The AMSR2 TBs were processed to provide consistent spatial resolution, and TB values were inter-calibrated. This product, "AMSR2 Daily Polar Gridded Sea Ice Concentrations, Version 2", NSIDC-0803 (Stewart et al., 2025; https://nsidc.org/data/nsidc-0803/versions/2), was released in 2025.

Comparison of AMSR2 NSIDC-0803 and SSMIS NSIDC-0051 Products

Here we compare the consistency of the AMSR2 NSIDC-0803 product with the legacy SSMIS NSIDC-0051 product. A three-year overlap period, 2023-2025, has been produced. This allows assessment over the annual cycle in both the Arctic and Antarctic, as well as some interannual variability.

Daily time series plots were produced that illustrate the extent and area differences between AMSR2 NSIDC-0803 and SSMIS NSIDC-0051. For comparison, the NRT SSMIS NSIDC-0081 extent and area differences were also plotted.

For Arctic extent (Figure 1), there is little bias in winter (January through March), but up to ~100,000-150,000 sq km low bias (NSIDC-0803 less than NSIDC-0051). The biases are similar for the NRT SSMIS, which indicates that the AMSR2 NSIDC-0803 product is similar in performance for the Arctic. The higher biases in summer are characteristic of previous passive microwave sensor transitions (Meier et al., 2011; Cavalieri et al., 2012) and are largely due to surface melt of the ice. In terms of percent difference, the low extent bias in summer amounts to 3-4% (Figure 2), slightly higher than SSMIS sensor transitions (Cavalieri et al., 2012); this is likely due to larger change from the different sensor, particularly the change in spatial resolution (even with resolution harmonization). Percentage differences are higher in summer also because the absolute extent is lower, so differences have a larger effect on the percentages.

For Antarctic extent (Figure 3), there are small biases in the austral autumn and early winter, and low biases up to ~200,000 sq km in late spring and early summer. The percent bias is small (0 to -0.5%) for March through November, then reaching an absolute. Underestimation by AMSR2 NSIDC-0803 relative to SSMIS NSIDC-0051 occurs December through February, peaking at -4 to -5% in late December through early January (Figure 4). The % biases are influenced by the strong seasonal cycle, where summer extents are small, which affects the percentage.

For the Arctic area (Figure 5), there is a consistent 100,000 to 200,000 sq km underestimation by AMSR2 NSIDC-0803 relative to SSMIS NSIDC-0051. This is larger than underestimation by the NRT SSMIS NSIDC-0081. This suggests concentration underestimation along with small biases in ice edge location. In terms of % difference (Figure 6), Arctic area bias reaches about 6% during summer and early autumn, likely related to surface melt and new ice formation. During winter, the % difference is about -1%.

The Antarctic area (Figure 7) shows a strong seasonal cycle in the AMSR2 NSIDC-0803 minus SSMIS NSIDC-0051 area, like the extent difference seasonal pattern, but of a greater magnitude. The area underestimation by AMSR2 NSIDC-0803 reaches -300,000 to -400,000 sq km during November to January. This is substantially more than the NRT SSMIS NSIDC-0081 bias, which has a maximum of ~150,000 sq km. In terms of percentage, the underestimation reaches -5% to -6% (Figure 8).

Example spatial maps of concentration differences are provided for the Arctic (Figure 9) and Antarctic (Figure 10) for representative dates where extent and area differences are largest. These maps show that the largest differences occur near the ice edge, which is expected. This is where there is high variability due to melt/growth and ice motion. It is also the regime most sensitive to spatial resolution. In the Arctic, the East Greenland Sea has particularly pronounced underestimation by AMSR2 NSIDC-0803, but other areas near the ice edge also show low biases. Within the ice pack, the biases are near zero. In the Antarctic, there is widespread underestimation by AMSR2 NSIDC-0803 around the entirety of the ice edge.

References

Cavalieri, D.J., C.L. Parkinson, N. DiGirolamo and A. Ivanoff (2012). Intersensor Calibration Between F13 SSMI and F17 SSMIS for Global Sea Ice Data Records," in *IEEE Geosci. Rem. Sens. Lett.*, 9(2), 233-236, http://doi.org/10.1109/LGRS.2011.2166754.

DiGirolamo, N., Parkinson, C. L., Cavalieri, D. J., Gloersen, P. & Zwally, H. J. (2022). Sea Ice Concentrations from Nimbus-7 SMMR and DMSP SSM/I-SSMIS Passive Microwave Data. (NSIDC-0051, Version 2). [Data Set]. Boulder, Colorado USA. NASA National Snow and Ice Data Center Distributed Active Archive Center. https://doi.org/10.5067/MPYG15WAA4WX.

Fetterer, F., Knowles, K., Meier, W. N., Savoie, M., Windnagel, A. K. & Stafford, T. (2025). Sea Ice Index. (G02135, Version 4). [Data Set]. Boulder, Colorado USA. National Snow and Ice Data Center. https://doi.org/10.7265/a98x-0f50.

Meier, W. N., Stewart, J. S., Wilcox, H., Hardman, M. A. & Scott, D. J. (2021). Near-Real-Time DMSP SSMIS Daily Polar Gridded Sea Ice Concentrations. (NSIDC-0081, Version 2). [Data Set]. Boulder, Colorado USA. NASA National Snow and Ice Data Center Distributed Active Archive Center. https://doi.org/10.5067/YTTHO2FJQ97K.

Meier, W.N., S.J.S. Khalsa, and M.H. Savoie (2011). Intersensor calibration between F-13 SSM/I and F-17 SSMIS near-real-time sea ice estimates, *IEEE Trans. Geosci. Rem. Sens.*, 49(9), 3343-3349, https://doi.org/10.1109/TGRS.2011.2117433.

Stewart, J. S., Meier, W. N., Marowitz, R., Scott, D. J. & Wilcox, H. (2025). AMSR2 Daily Polar Gridded Sea Ice Concentrations. (NSIDC-0803, Version 2). [Data Set]. Boulder, Colorado USA. National Snow and Ice Data Center. https://doi.org/10.5067/W13AO54SS7CW

Figures

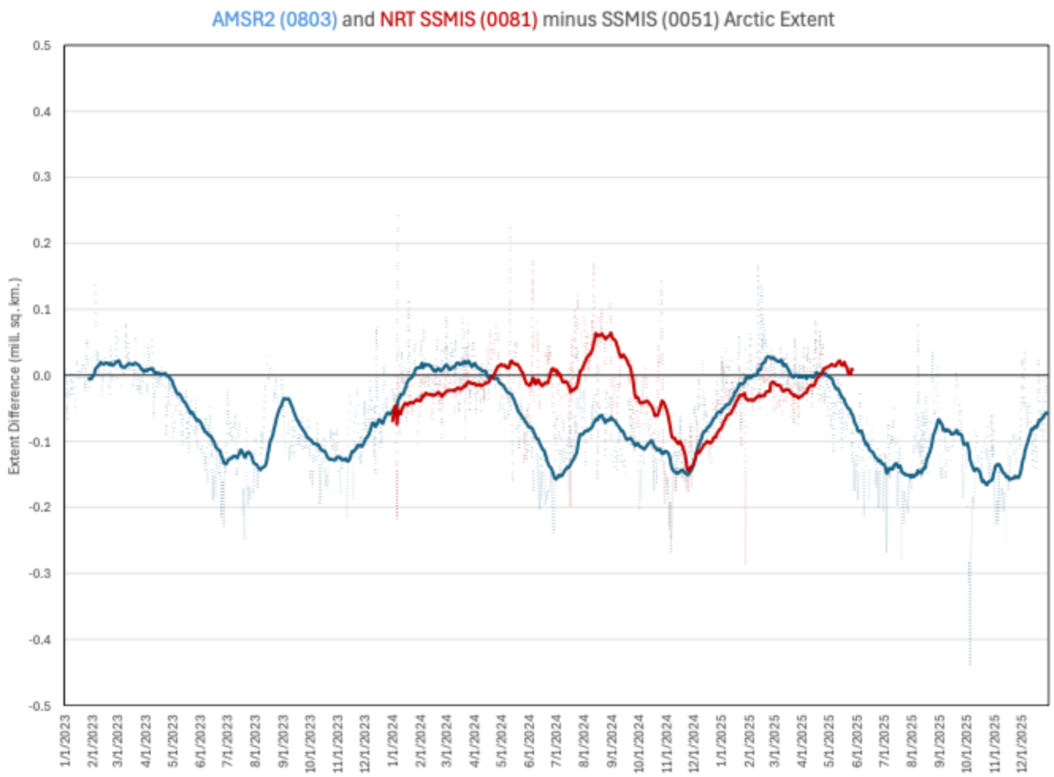

Figure 1. Arctic sea ice extent difference for AMSR2 (0803) minus SSMIS (0051) (blue) for 2023 through 2025, and NRT SSMIS (0081) minus SSMIS (0051) (red) for 2024 to May 2025. Dotted lines are daily extent values and solid lines are 28-day running averages.

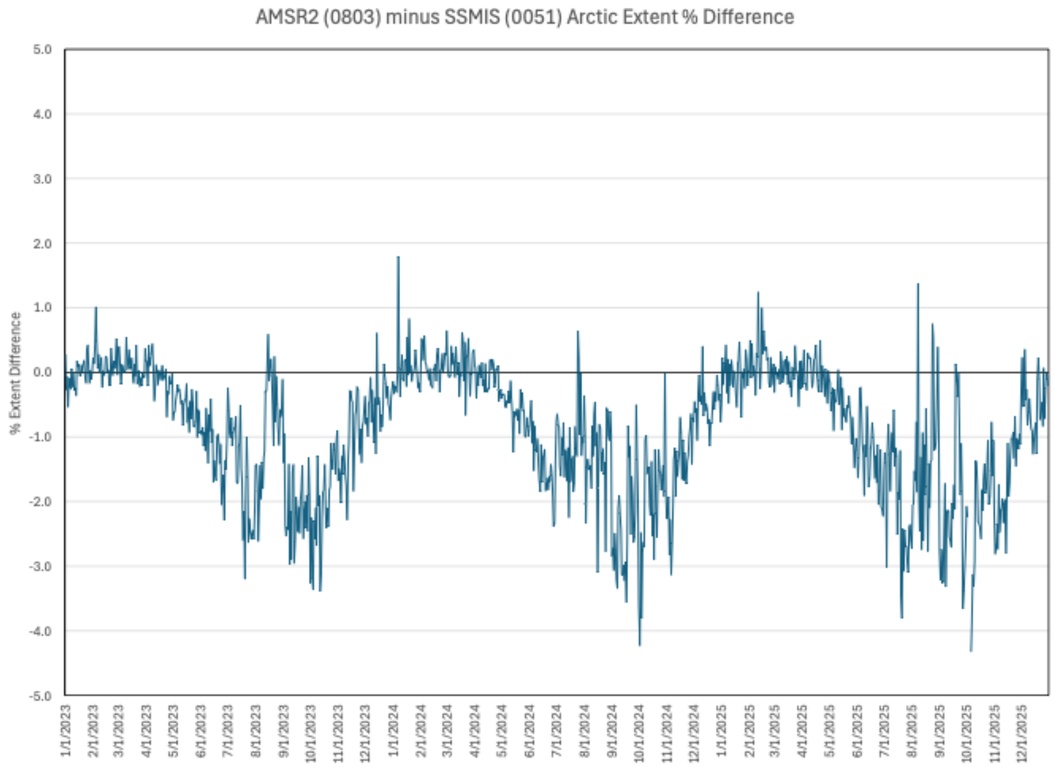

Figure 2. Arctic sea ice extent % difference for AMSR2 (0803) minus SSMIS (0051) for 2023 through 2025.

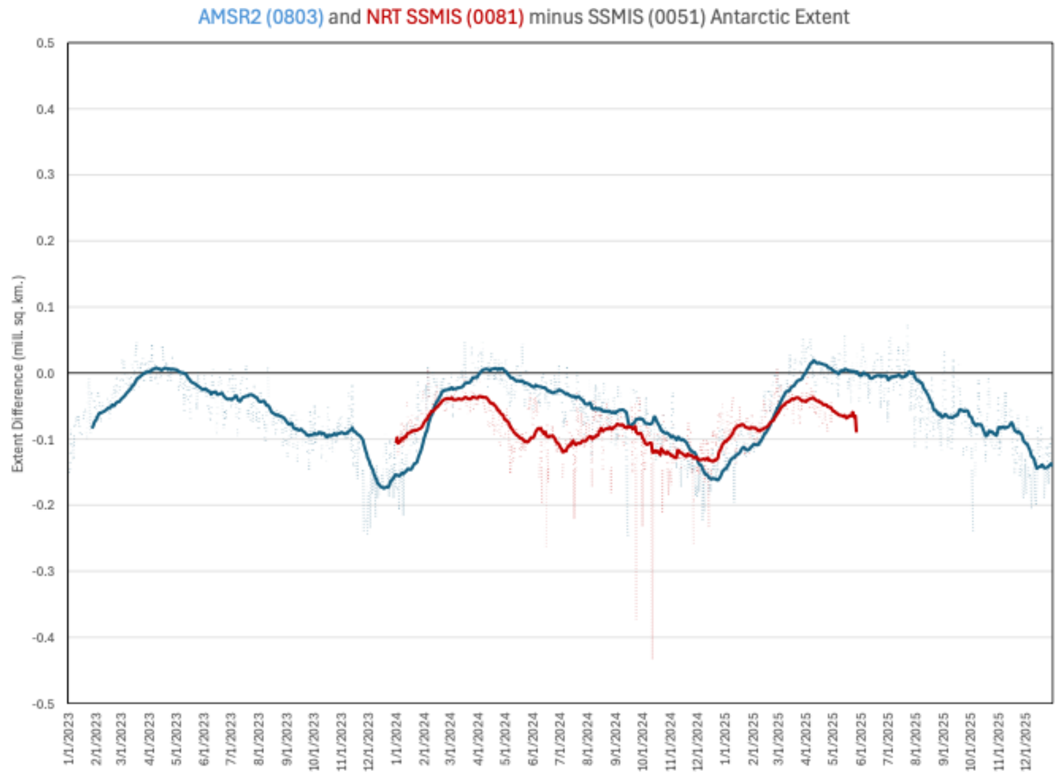

Figure 3. Antarctic sea ice extent difference for AMSR2 (0803) minus SSMIS (0051) (blue) for 2023 through 2025, and NRT SSMIS (0081) minus SSMIS (0051) (red) for 2024 to May 2025. Dotted lines are daily extent values and solid lines are 28-day running averages.

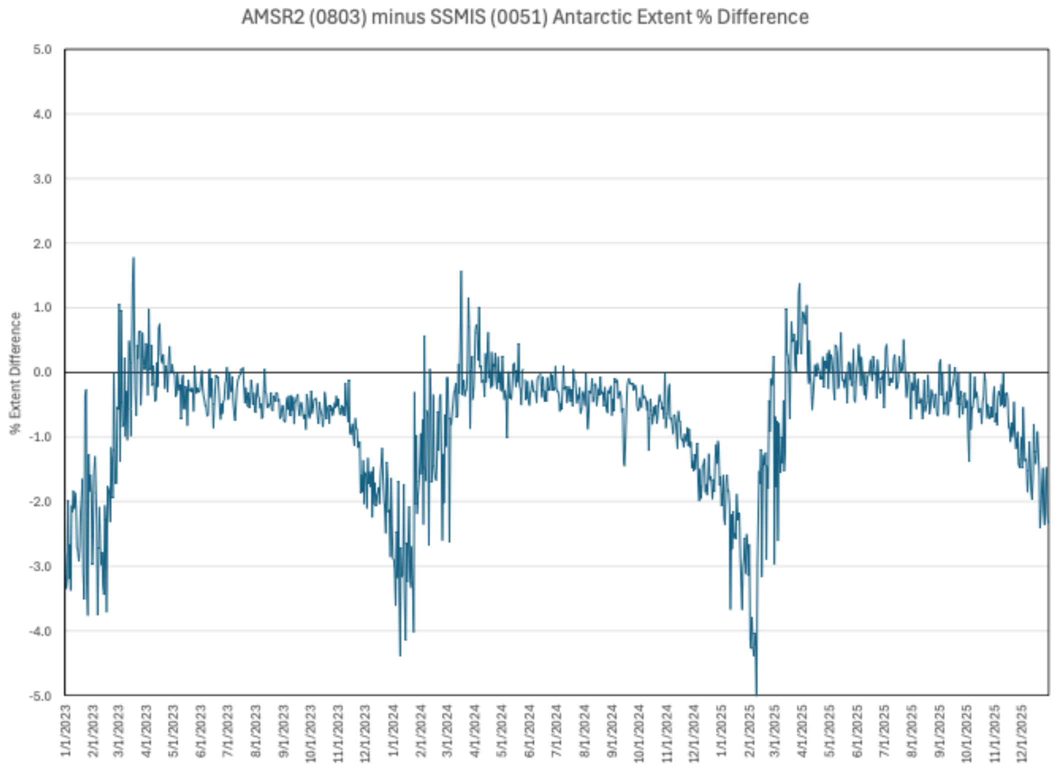

Figure 4. Antarctic sea ice extent % difference for AMSR2 (0803) minus SSMIS (0051) for 2023 through 2025.

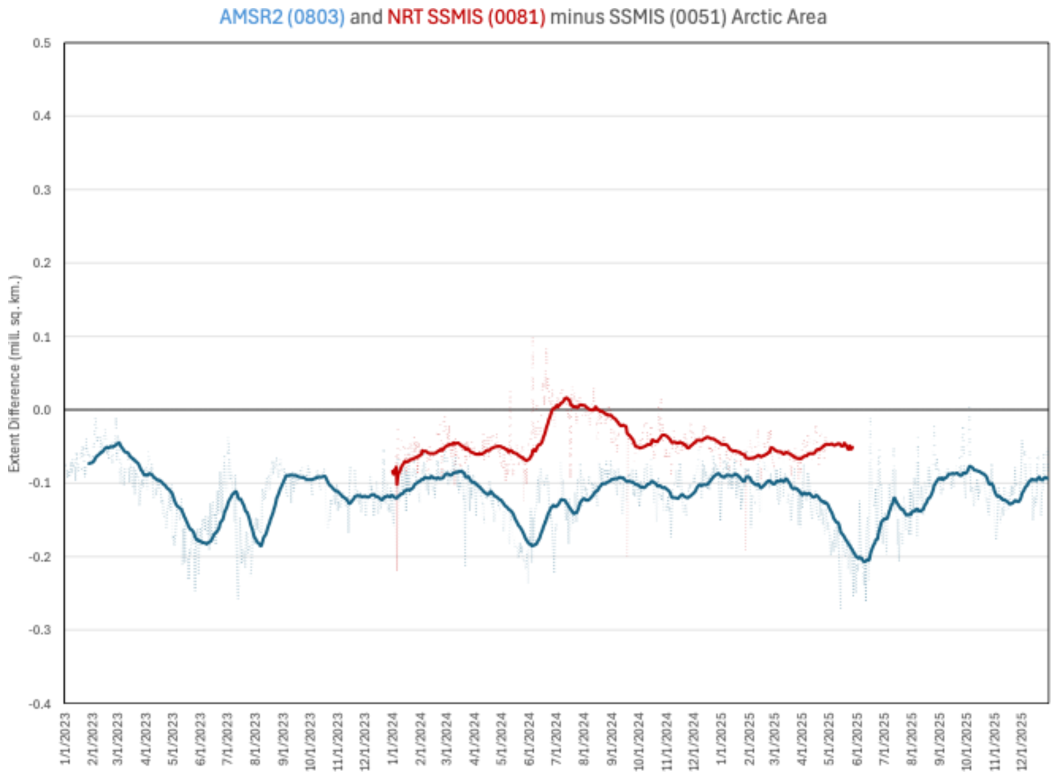

Figure 5. Arctic sea ice area difference for AMSR2 (0803) minus SSMIS (0051) (blue) for 2023 through 2025, and NRT SSMIS (0081) minus SSMIS (0051) (red) for 2024 to May 2025. Dotted lines are daily extent values and solid lines are 28-day running averages.

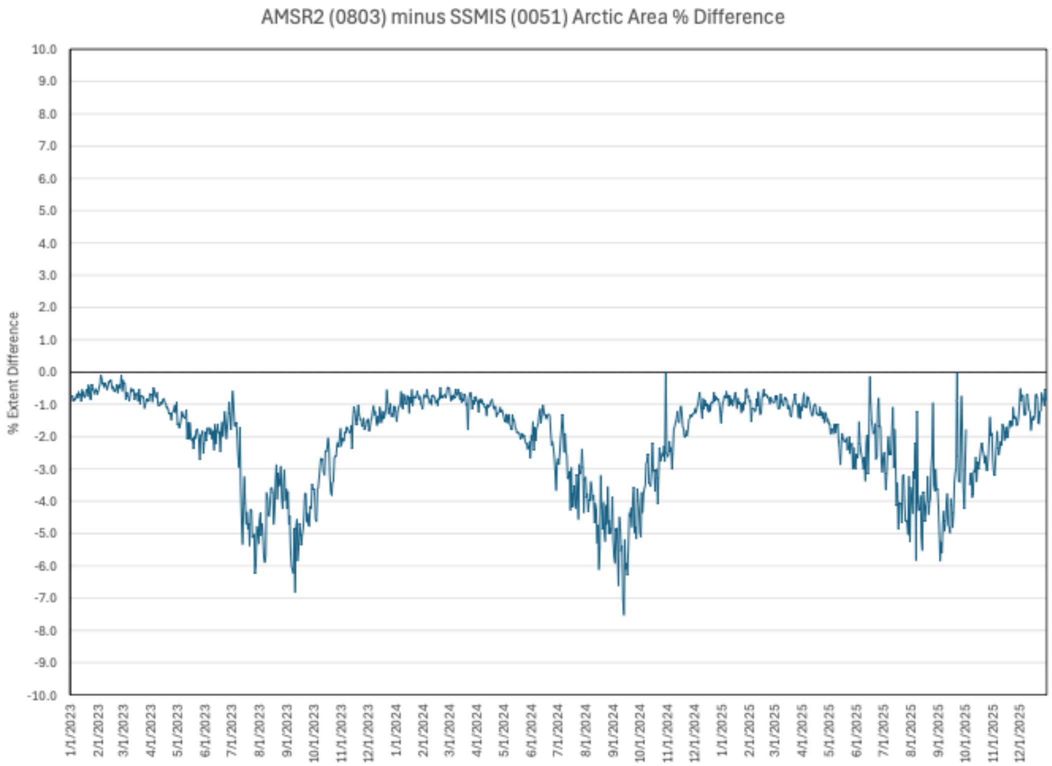

Figure 6. Arctic sea ice area % difference for AMSR2 (0803) minus SSMIS (0051) for 2023 through 2025.

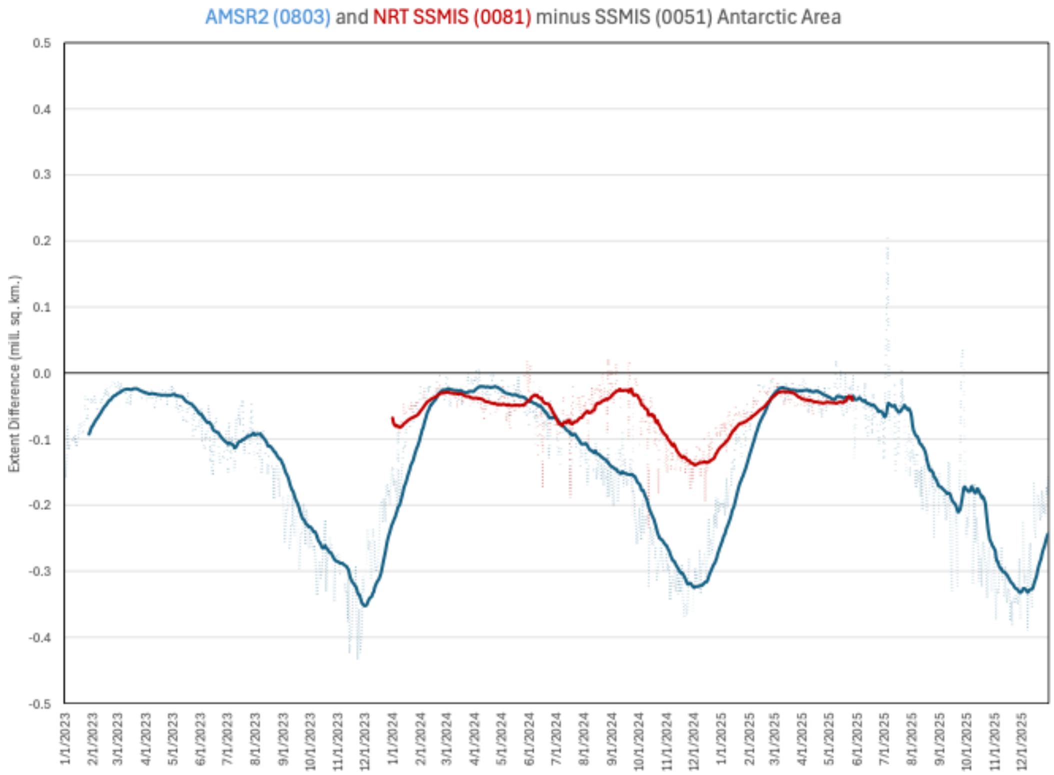

Figure 7. Antarctic sea ice area difference for AMSR2 (0803) minus SSMIS (0051) (blue) for 2023 through 2025, and NRT SSMIS (0081) minus SSMIS (0051) (red) for 2024 to May 2025. Dotted lines are daily extent values and solid lines are 28-day running averages.

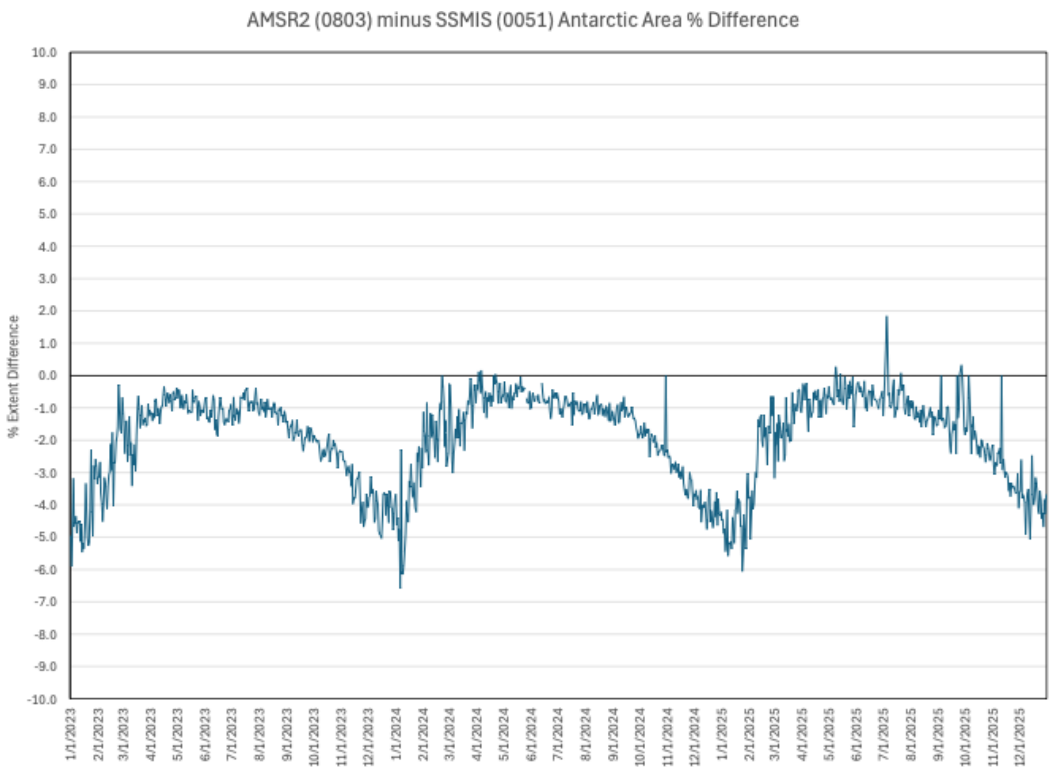

Figure 8. Antarctic sea ice area % difference for AMSR2 (0803) minus SSMIS (0051) for 2023 through 2025.

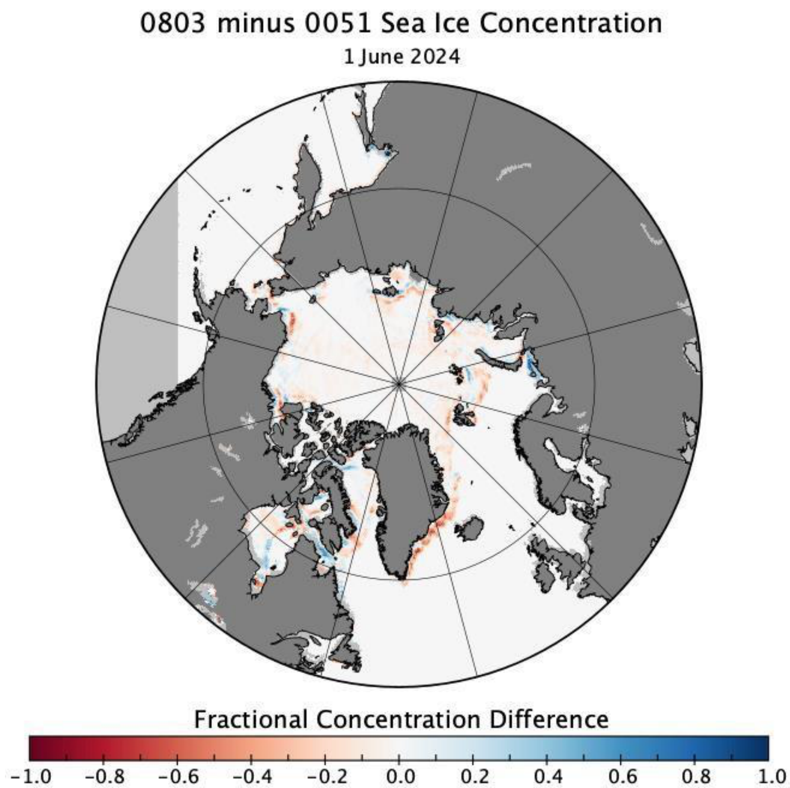

Figure 9. Arctic AMSR2 0803 minus SSMIS 0051 concentration difference map for 1 June 2024, representative of when differences are largest, during summer.

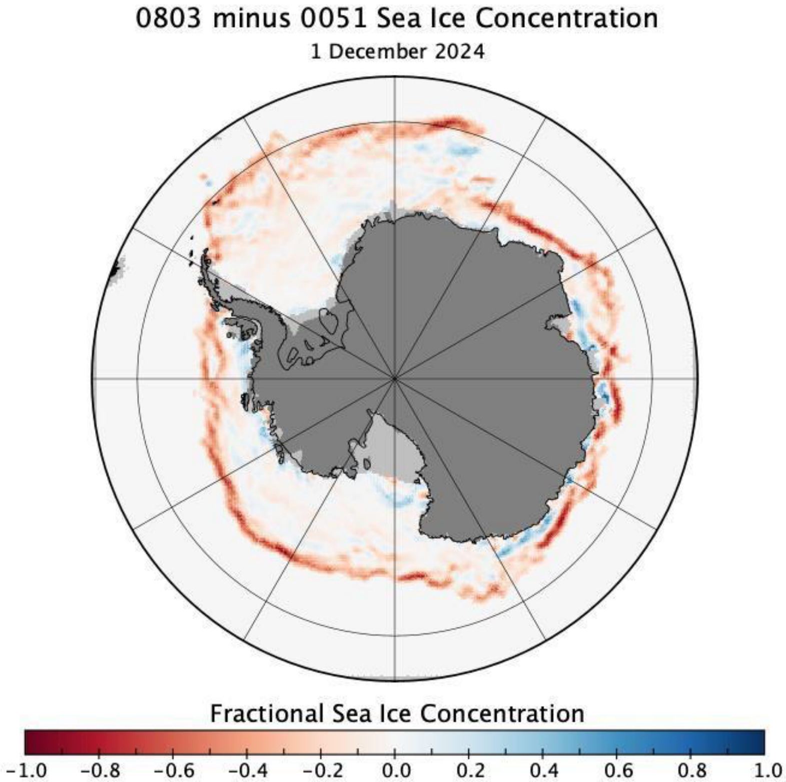

Figure 10. Antarctic AMSR2 0803 minus SSMIS 0051 concentration difference map for 1 December 2024, representative of when differences are largest, during summer.